CDF/PUB/EXOTIC/PUBLIC/9730

Search for diboson (W^+W^- or $W^\pm Z^\circ$) resonances in electron, missing $\mathbf{E}_T$ and two jets final state.

The CDF Collaboration
URL http://www-cdf.fnal.gov
(Dated: April 6, 2009)

Based on 2.9 fb^{-1} data we report on a search for resonances decaying into a pair of gauge bosons, W^+W^- or $W^\pm Z^\circ$. In this search mode, one W decays through a leptonic (electron) mode and the other boson decays into two jets. Without any excess above the expected standard model background, three resonance hypotheses, G* (R/S graviton), Z' and W', are tested and their cross section limits at 95% confidence level are calculated. Comparing the limits to their theoretical cross sections, the mass exclusion regions for the three particles are set.

I. INTRODUCTION

This note describes a search for beyond standard model (SM) particles in the form of diboson resonances where one boson decays to electron and neutrino (missing E_T) and the other decays to two jets. This final state has the advantage of searching for two types of diboson resonances, W^+W^- and $W^{\pm}Z^{\circ}$, with the same final state. The hadronic decay of the W or Z to two jets has the advantage of a higher branching fraction compared to the leptonic mode. However, background from jets also increases. In this analysis we implement a series of cuts as a function of E_T to reduce standard model backgrounds and enhance sensitivity.

II. DATA SAMPLE & EVENT SELECTION

This analysis is based on an integrated luminosity of 2.9 fb^{-1} collected with the CDFII detector between March 2002 and February 2008. The CDF detector is described in detail in [1]. The data are collected with an inclusive electron trigger that requires a central electron with $E_T > 18$ GeV. From this dataset we select events with an isolated electron ($E_T > 30$ GeV), a missing $E_T > 30$ GeV, 2 or 3 jets with $|\eta| < 2.5$ and $E_T > 30$ GeV, and an overall $H_T > 150$ GeV. H_T is defined as the sum of the electron E_T, the missing E_T and the jet E_T of all jets with raw $E_T > 8$ GeV.

III. EVENT RECONSTRUCTION

To reconstruct WW or WZ from selected events, the electron and missing E_T are first combined to form a W. Because missing E_Z is not available, the invariant mass of the electron and missing E_T is artificially set to the W mass. With this assumption, the conservation of energy and momentum results in a quadratic equation for missing E_Z and there are usually two solutions for missing E_Z. If the discriminant is negative, the combination is discarded, while for the positive case, both solutions are kept.

Two jets are combined to form W or Z. In the case of W, we require the 2-jet invariant mass (M_{jj}) to fall between 65 and 95 GeV, corresponding to $\pm 1.5\sigma$ of the reconstructed W. In the case of Z, this window is between 70 and 105 GeV. For a three jet event there are three invariant mass combinations. In this case only the pair closest to either the W or the Z mass is chosen in order to reduce the combinatorial background.

The reconstructed W or Z candidates are then combined to form a final WW or WZ invariant mass. We further impose $|\eta| < 4.0$ on the η of the reconstructed resonance to reduce the possible beam jet effect.

IV. BACKGROUNDS

The backgrounds considered for this analysis are 12 standard model processes listed in Figure 1 and Figure 2. The dominating background is the W + jets events which accounts for $\sim 60\%$ of the overall background with the event selection criteria described in section II. The W + jets background is estimated using the ALPGEN [2] event generator interfaced with Pythia as parton shower. Other than W+jets and QCD processes, the rest are generated using the Pythia [3] event generator.

Of the 12 backgrounds, QCD jet background is the only process not estimated with Monte Carlo data. When a QCD jet event has more than three jets and one of the jets is misidentified as an electron, the event may pass through subsequent selection criteria and reconstruction processes.

The QCD background is estimated using the jet data sets. We first exclude events with at least one tight electron. Then, each jet in the central region is treated as an electron with a weight corresponding to the fake rate probability as a function of jet E_T. The fake rate is from an earlier analysis [6] and varies from $\sim 10^{-4}$ at 30 GeV to $\sim 10^{-3}$ above 100 GeV. This fake electron is used in the subsequent WW or WZ reconstruction process as described in section III. The QCD background is normalized to the data in a low missing E_T region, where no signal is expected: the scale factor is estimated using the missing E_T spectrum for events with 2 jets in the final state, and comparing the total backgrounds with the data.

Figure 1 and Figure 2 show the reconstructed invariant mass distributions before E_T cut optimization for WW and WZ respectively with data overlaying backgrounds. The composition of the background processes is listed next to the figures. QCD jet contributes $\sim 11\%$ in both cases.

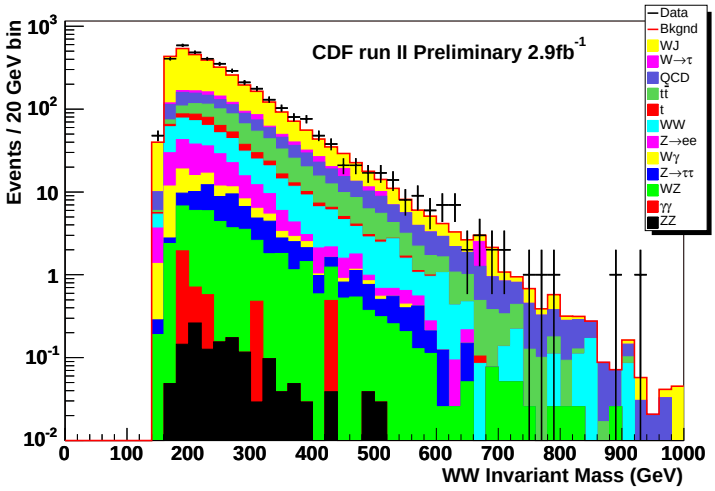

X → WW → e ν q q						
BG process	Events	±	stat	±	sys	Fraction
W(→eν) + jet	1959.8	±	15.3	±	393.4	58.52%
QCD bg	359.4	±	4.8	±	71.9	10.73%
t tbar	316.9	±	2.3	±	30.9	9.46%
WW	259.6	±	4.7	±	36.8	7.75%
Z(→ee) + jet	139.8	±	3.1	±	60.4	4.17%
W(→τν) + jet	102.1	±	11.4	±	13.2	3.05%
Single top	86.2	±	1.3	±	12.2	2.57%
WZ	41.4	±	1.0	±	4.0	1.24%
Wγ	40.6	±	1.3	±	7.8	1.21%
Z→ττ	38.3	±	1.9	±	9.4	1.14%
γγ	3.6	±	1.3	±	2.7	0.11%
ZZ	1.4	±	0.1	±	0.2	0.04%
W(→μν) + jet	0	±	0	±	0	0%
Total BG	3349.0	±	20.9	±	513.7	100.00%
Observed Data	3577.0	±	59.8			

CDF Run II Preliminary. $\int L\,dt = 2.9\,fb^{-1}$

FIG. 1: Left: Reconstructed WW invariant mass before E_T cut optimization. Data overlaying background stack-up. Right: Data and breakdown of the background composition

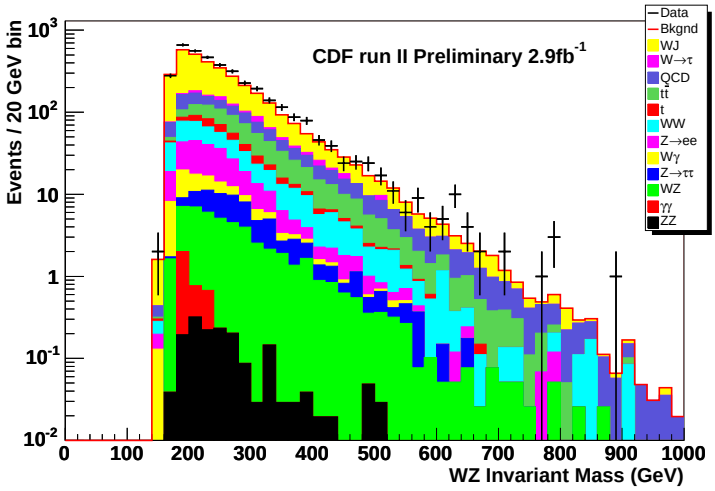

X → WZ → e ν q q						
BG process	Events	±	stat	±	sys	Fraction
W(→eν) + jet	1977.4	±	15.5	±	389.1	58.96%
QCD bg	361.2	±	4.8	±	72.2	10.77%
t tbar	329.5	±	2.4	±	32.0	9.82%
WW	226.1	±	4.4	±	48.8	6.74%
Z(→ee) + jet	153.9	±	3.2	±	60.3	4.59%
Single top	91.4	±	1.3	±	13.3	2.72%
W(→τν) + jet	85.5	±	10.4	±	16.2	2.55%
WZ	45.6	±	1.1	±	6.5	1.36%
Wγ	42.3	±	1.4	±	8.2	1.26%
Z→ττ	36.7	±	1.9	±	9.4	1.10%
γγ	2.7	±	1.1	±	1.9	0.08%
ZZ	1.7	±	0.1	±	0.3	0.05%
W(→μν) + jet	0	±	0	±	0	0%
Total BG	3354.0	±	20.4	±	535.3	100.00%
Observed Data	3735.0	±	61.1			

CDF Run II Preliminary. $\int L\,dt = 2.9\,fb^{-1}$

FIG. 2: Left: Reconstructed WZ invariant mass before E_T cut optimization. Data overlaying background stack-up. Right: Data and breakdown of the background composition

V. SIGNAL DETECTION EFFICIENCY

Signal detection efficiency is evaluated using Monte Carlo data simulated with the Pythia event generator and CDF-SIM, the CDF detector simulation. For a set of selected mass values, 3 types of particles are generated: R/S graviton, G*, with k/m_p=0.1, and the sequential Z' and W' with standard model coupling constants. The reconstructed signal is a Gaussian shape, and the mass resolution is linearly proportional to the generated mass values, varying from 15 GeV at 200 GeV mass to 55 GeV at 700 GeV mass. In order to calculate the efficiency we choose a mass window $\pm 1.5\sigma$ of the reconstructed signal and rounded to 5 GeV for histogram binning. This choice is somewhat ad hoc but gives a good signal to background ratio. The same acceptance windows are used to obtain the number of background events.

VI. OPTIMIZATION OF CUTS

In order to improve sensitivities at higher mass regions, additional higher E_T cuts for constituent particles (electron, missing E_T, jets) are applied. Two series of E_T cuts are implemented: One is to require a higher E_T on all 4 participant particles ranging from 40 GeV to 80 GeV in 10 GeV steps. The other is to require a higher E_T on one of each boson's decay daughters, namely, higher E_T for either the electron or the missing E_T ($W \to e\nu$) and the same higher E_T for one of the two jets ($W/Z \to jj$). The increased value of E_T runs from 40 to 120 GeV in 10 GeV steps. These 2 sets of cuts make up a total of 15 variations of E_T cuts including the original $E_T > 30$ GeV cut described in section II. The systematic and statistical errors are re-calculated for all variations. The expected cross section limits are calculated for each of the 15 cuts at each selected mass value and the cut that gives the best expected limit is chosen for the final result (see section VIII).

VII. SYSTEMATIC UNCERTAINTIES

The systematic uncertainties included in the background processes are listed in decreasing significance:

- Jet Energy Scale uncertainty (JES)
- Cross section uncertainty
- Jet fake rate uncertainty
- Luminosity uncertainty

The dominating uncertainty is JES uncertainty ($\sim 13\%$). The cross section and luminosity uncertainties are $\sim 6\%$ each.

The systematic uncertainties considered in the signal acceptance are the following, also listed in decreasing significance:

- Jet Energy Scale uncertainty (JES)
- Luminosity uncertainty (6%)
- Initial State Radiation uncertainty (ISR)
- Final State Radiation uncertainty (FSR)
- Parton Distribution Function uncertainty (PDF)

The dominating uncertainty is still the JES uncertainty which varies from 12% at 170 GeV mass to 6% at 700 GeV mass for G*, 13% (170 GeV) to 5% (700 GeV) for Z', and 9% (190 GeV) to 6% (700 GeV) for W'.

VIII. CROSS SECTION LIMIT CALCULATION

Without any evidence of excess, a Bayesian method is used to calculate 95% confidence level cross section limits. The calculation uses signal acceptance (signal detection efficiency $\times$ integrated luminosity), estimated background, and observed data as inputs. The acceptance and background priors are modeled via a Monte Carlo method which allows implementation of correlations between acceptances and backgrounds. In our analysis the JES and luminosity uncertainties in the acceptance and the background are correlated.

In addition to cross section limits calculated from observed data, expected 95% CL limits are calculated from pseudo experiments with the pseudo data simulated from the background distribution.

IX. RESULTS

Table I lists the resulting optimal cuts for each of the three particle types. Figure 3 shows G* cross section limits from the optimal E_T cuts and the ratio relative to the reference theoretical cross section. The theoretical cross section of G* is calculated from Pythia 6.216 and a constant k factor of 1.3 is applied in order to take into account the NLO correction [4]. After appling the optimal E_T cut for 600 GeV G* (2,120), the WW invariant mass distribution comparing the total background and the data is plotted in Figure 4. Also shown in the figure is the expected 600 GeV G* signal with the optimal cut. The background composition for this particular cut is listed in Table II.

Mass (GeV)	165	170	190	250	300	350	400	450	500	600	700
G* Optimal Cut	2,40	2,40	2,50	2,60	4,50	2,80	2,90	4,50	2,110	2,120	2,120
Z' Optimal Cut	2,40	2,40	2,40	4,40	4,50	4,50	4,60	4,60	4,60	4,60	4,60
W' Optimal Cut	-	-	2,40	4,40	4,50	4,50	4,60	4,60	4,60	4,60	4,60

TABLE I: Optimal E_T cuts applied to G*, Z' and W'. Here "2,40" stands for "(E_T(electron) or missing E_T) > 40 GeV, and, (E_T(jet1) or E_T(jet2)) > 40 GeV" and "4,40" stands for "(E_T(electron) and missing E_T and E_T(jet1) and E_T(jet2)) > 40 GeV".

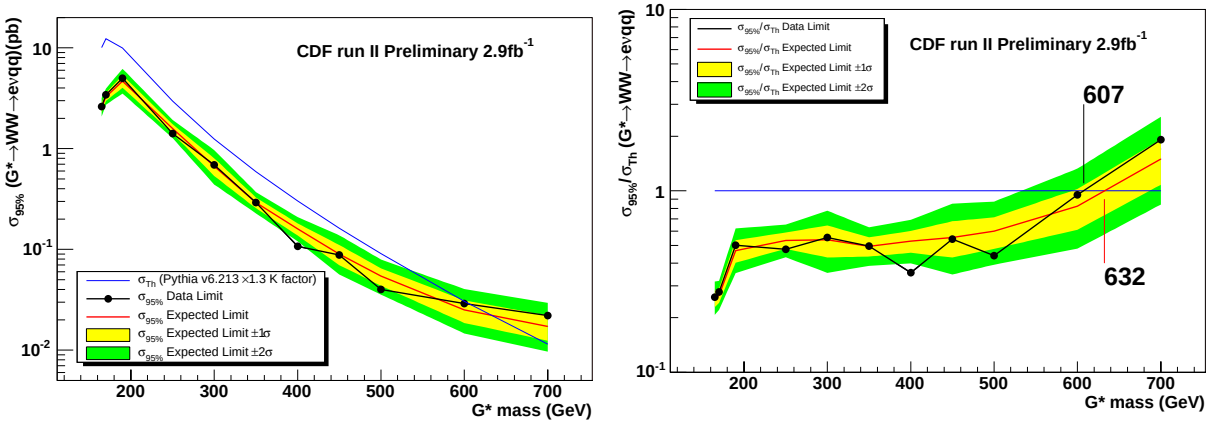

FIG. 3: Left: 95% CL cross section limit for G*(k/m_p=0.1). Red line is expected limit. Yellow band is $\pm 1\sigma$ of expected limit. Green band is $\pm 2\sigma$ of expected limit. Black line with dots is data limit. Blue line is theoretical cross section of G* from Pythia 6.216 and using a constant k factor 1.3 [4]. Right: Cross section limits divided by theoretical cross section. Mass regions with ratio below 1 are excluded. Expected cross section limits exclude G* mass region < 632 GeV. Observed data limits exclude mass region < 607 GeV.

Figure 5 shows Z' cross section limits from the optimal E_T cuts and the ratio relative to the reference theoretical cross section. The Z' theoretical cross section is also from Pythia 6.216 with a constant k factor 1.3 for NLO contribution [5, 6]. The WW invariant mass distribution for the optimal E_T cut for 600 GeV Z' (4,60) is shown in Figure 6 with the expected 600 GeV Z' signal. The optimal E_T cut for G* and Z' at the same mass value are different although both of them are WW resonances. The corresponding background composition is listed in Table III.

Figure 7 shows W' cross section limits from the optimal E_T cuts and the ratio relative to the reference theoretical cross section. The W' theoretical cross section in comparison is derived from a NLO calculation in [7]. The WZ invariant mass distribution for the optimal E_T cut at 600 GeV (4,60) is shown in Figure 8 with the expected 600 GeV W' signal. Although the optimal E_T cut for W' is the same as Z', they are different distributions: WZ as opposed to WW. The corresponding background composition is shown in Table IV.

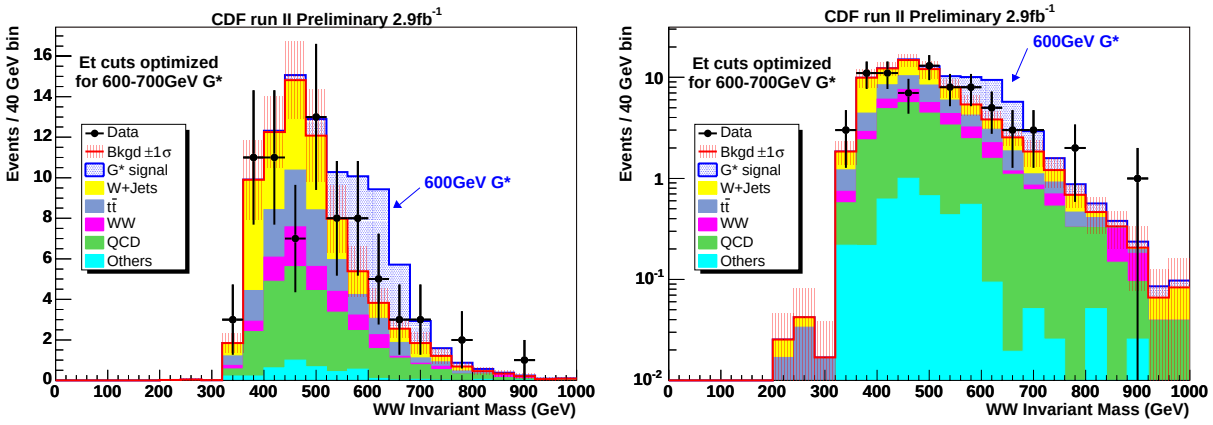

FIG. 4: G* search. Background and data with the optimal E_T cuts for 600 GeV G* . Expected G* signal at 600 GeV is added on top of the background. Left: In linear scale. Right: In log scale.

G* → W W → e ν q q		
BG Process	Events ± stat. ± sys.	Fraction
QCD bg	24.72 ± 0.18 ± 4.94	32.70%
W(→eν)+jet	21.46 ± 1.32 ± 5.60	28.38%
tt̄	14.79 ± 0.50 ± 2.00	19.56%
WW	8.10 ± 0.83 ± 2.25	10.71%
W(→ τν)+jet	2.55 ± 1.80 ± 1.31	3.37%
WZ	1.31 ± 0.18 ± 0.24	1.73%
Z(→ee)+jet	1.16 ± 0.28 ± 0.45	1.53%
Single top	0.82 ± 0.13 ± 0.11	1.08%
Z → ττ	0.59 ± 0.24 ± 0.15	0.78%
Wγ	0.09 ± 0.06 ± 0.04	0.11%
ZZ	0.04 ± 0.02 ± 0.00	0.05%
γγ	0.00 ± 0.00 ± 0.00	0.00%
W(→ μν)+jet	0.00 ± 0.00 ± 0.00	0.00%
Total BG	75.62 ± 2.48 ± 11.23	100.00%
Observed Data	75 ± 8.7	

TABLE II: Data and background composition of WW invariant mass in Figure 4.

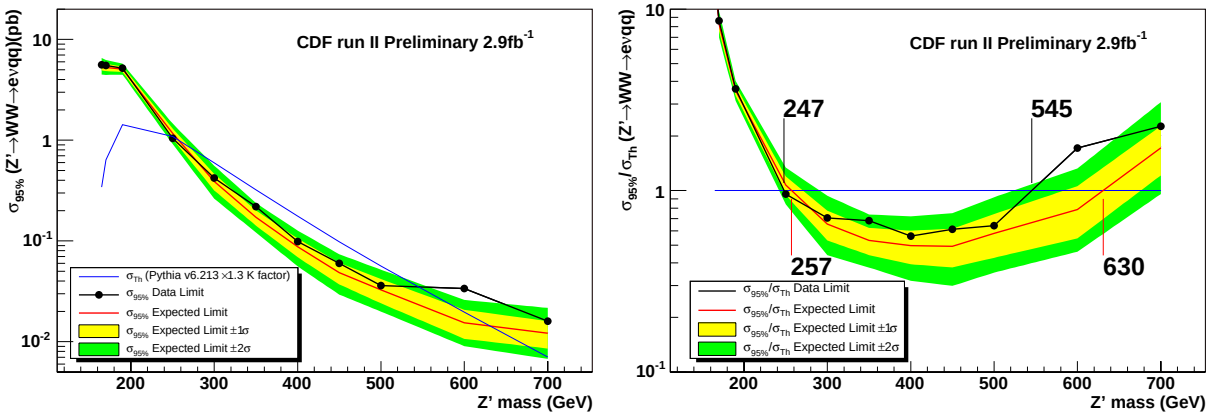

FIG. 5: Left: 95% CL cross section limit for Z'. Red line is expected limit. Yellow band is $\pm 1\sigma$ of expected limit. Green band is $\pm 2\sigma$ of expected limit. Black line with dots is data limit. Blue line is theoretical cross section of SM Z' from Pythia 6.216 and using a constant k factor 1.3 [5, 6]. Right: Cross section limits divided by theoretical cross section. Mass regions with ratio below the horizontal line at 1 are excluded. Expected cross section limits exclude mass region 257 GeV $< M_{Z'} <$630 GeV. Observed data limits exclude mass region 247 GeV $< M_{Z'} <$ 545 GeV.

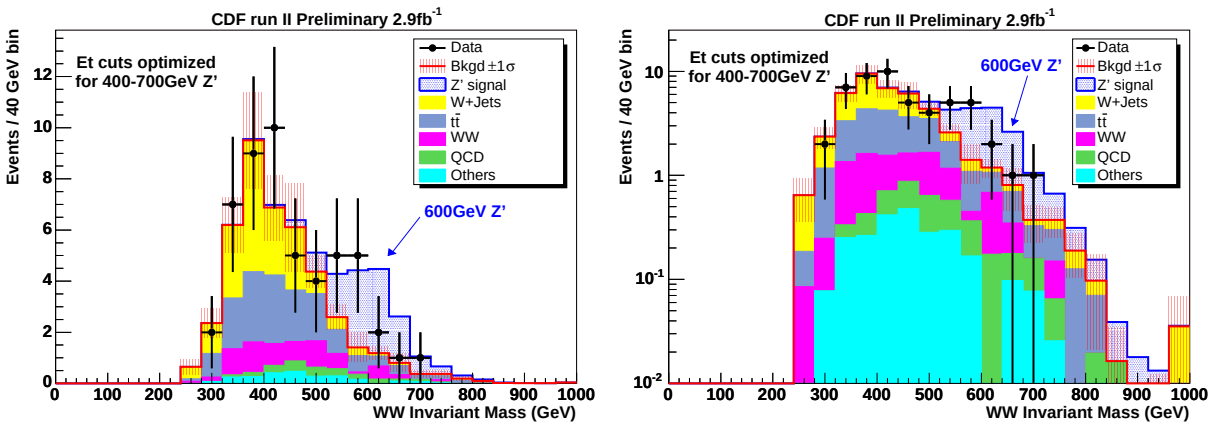

FIG. 6: Z' search. Background and data with the E_T cut optimal for 600 GeV Z'. Expected Z' signal at 600 GeV is added on top of the background. Left: In linear scale. Right: In log scale.

Z' → W W → e ν q q		
BG Process	Events ± stat. ± sys.	Fraction
$t\bar{t}$	15.13 ± 0.51 ± 1.64	35.05%
W(→eν)+jet	14.26 ± 1.11 ± 3.76	33.04%
WW	6.56 ± 0.75 ± 0.96	15.21%
W(→ τν)+jet	2.55 ± 1.80 ± 0.30	5.91%
QCD bg	2.21 ± 0.06 ± 0.44	5.13%
WZ	1.03 ± 0.16 ± 0.16	2.38%
Z → ττ	0.68 ± 0.26 ± 0.06	1.58%
Single top	0.54 ± 0.10 ± 0.07	1.26%
Z(→ee)+jet	0.14 ± 0.10 ± 0.14	0.32%
ZZ	0.05 ± 0.02 ± 0.01	0.11%
γγ	0.00 ± 0.00 ± 0.00	0.00%
Wγ	0.00 ± 0.00 ± 0.00	0.00%
W(→ μν)+jet	0.00 ± 0.00 ± 0.00	0.00%
Total BG	43.16 ± 2.33 ± 5.68	100.00%
Observed Data	51 ± 7.1	

TABLE III: Data and background composition of WW invariant mass in Figure 6.

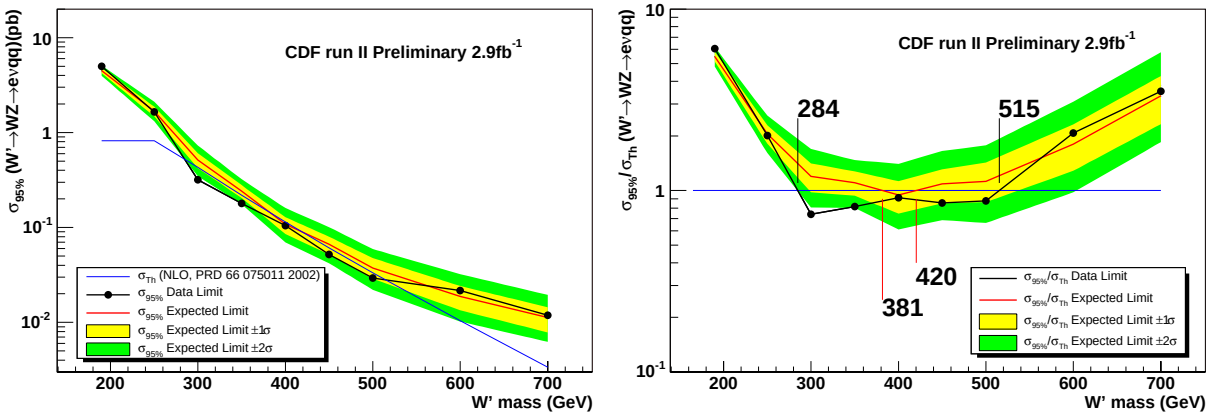

FIG. 7: Left: 95% CL cross section limit for W'. Red line is expected limit. Yellow band is $\pm 1\sigma$ of expected limit. Green band is $\pm 2\sigma$ of expected limit. Black line with dots is data limit. Blue line is theoretical cross section of W' from a NLO calculation [7]. Right: Cross section limits divided by theoretical cross section. Mass regions with ratio below 1 are excluded. Expected cross section limits exclude mass region 381 GeV $< M_{W'} <$420 GeV. Observed data limits exclude mass region 284 GeV $< M_{W'} <$ 515 GeV.

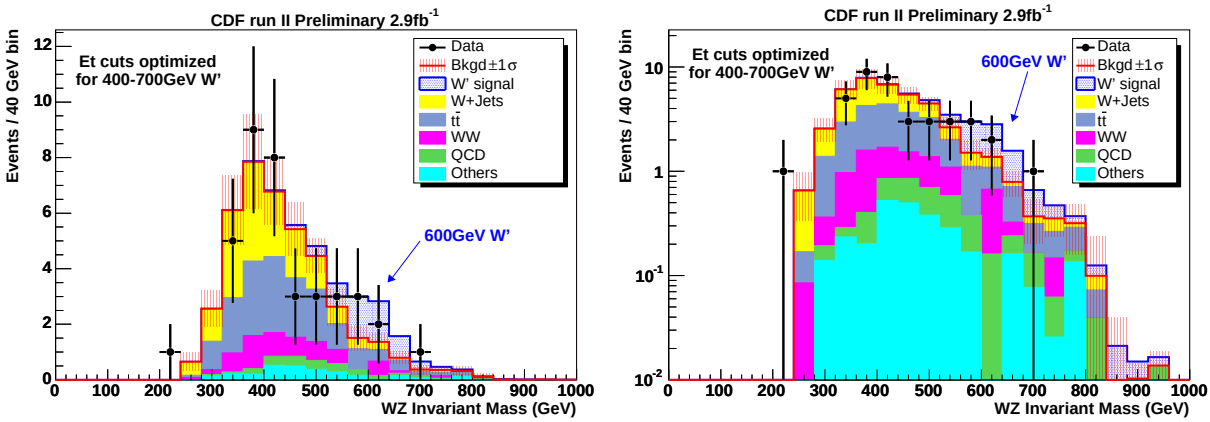

FIG. 8: W' search. Background and data with the E_T cut optimal for 600 GeV W'. Expected W' signal at 600 GeV is added on top of the background. Left: In linear scale. Right: In log scale.

W' → W Z → e ν q q		
BG Process	Events ± stat. ± sys.	Fraction
$t\bar{t}$	15.45 ± 0.51 ± 2.09	37.38%
W(→eν)+jet	15.21 ± 1.14 ± 3.85	36.80%
WW	5.54 ± 0.69 ± 1.13	13.41%
QCD bg	2.29 ± 0.07 ± 0.46	5.55%
WZ	1.41 ± 0.19 ± 0.13	3.42%
Z → $\tau\tau$	0.59 ± 0.24 ± 0.06	1.42%
Single top	0.50 ± 0.10 ± 0.09	1.22%
Z(→ee)+jet	0.14 ± 0.10 ± 0.10	0.33%
Wγ	0.13 ± 0.07 ± 0.09	0.31%
ZZ	0.07 ± 0.03 ± 0.01	0.16%
$\gamma\gamma$	0.00 ± 0.00 ± 0.00	0.00%
W(→ $\tau\nu$)+jet	0.00 ± 0.00 ± 0.00	0.00%
W(→ $\mu\nu$)+jet	0.00 ± 0.00 ± 0.00	0.00%
Total BG	41.33 ± 1.47 ± 6.88	100.00%
Observed Data	38 ± 6.2	

TABLE IV: Data and background composition of WZ invariant mass in Figure 8.

X. CONCLUSIONS

We present a search for new particles decaying into a pair of bosons in the electron, missing E_T and two jets final state. With an integrated luminosity of 2.9 fb^{-1}, no significant excess over the standard model prediction is observed. Without any excess, the cross section limits at 95% CL are obtained for R/S graviton, standard model Z' and W' as a function of mass. By comparing the limits with theoretical cross sections, the mass exclusion regions are derived and listed in Table V.

	G*	Z'	W'
Expected Exclusion	< 632 GeV	257 - 630 GeV	381-420 GeV
Data Exclusion	< 606 GeV	247 - 545 GeV	284-515 GeV

TABLE V: Mass exclusion region.

Acknowledgments

We thank the Fermilab staff and the technical staffs of the participating institutions for their vital contributions. This work was supported by the U.S. Department of Energy and National Science Foundation; the Italian Istituto Nazionale di Fisica Nucleare; the Ministry of Education, Culture, Sports, Science and Technology of Japan; the Natural Sciences and Engineering Research Council of Canada; the National Science Council of the Republic of China; the Swiss National Science Foundation; the A.P. Sloan Foundation; the Bundesministerium fuer Bildung und Forschung, Germany; the Korean Science and Engineering Foundation and the Korean Research Foundation; the Particle Physics and Astronomy Research Council and the Royal Society, UK; the Russian Foundation for Basic Research; the Comision Interministerial de Ciencia y Tecnologia, Spain; and in part by the European Community's Human Potential Programme under contract HPRN-CT-20002, Probe for New Physics.

[1] F. Abe, et al., Nucl. Instrum. Methods Phys. Res. A **271**, 387 (1988); D. Amidei, et al., Nucl. Instum. Methods Phys. Res. A **350**, 73 (1994); F. Abe, et al., Phys. Rev. D **52**, 4784 (1995); P. Azzi, et al., Nucl. Instrum. Methods Phys. Res. A **360**, 137 (1995); The CDFII Detector Technical Design Report, Fermilab-Pub-96/390-E
[2] M.L. Mangano, M. Moretti, F. Piccinini, R. Pittau, A. Polosa, ALPGEN, a generator for hard multiparton processes in hadronic collisions, JHEP **0307**, 001 (2003).
[3] T. Sjostrand et al., High-Energy-Physics Event Generation with PYTHIA 6.1, Comput. Phys. Commun. **135**, 238 (2001).
[4] T. Aaltonen, *et al* (CDF collaboration), Phys. Rev. Lett. **99**, 171801 (2007).
[5] T. Aaltonen, *et al* (CDF collaboration), Phys. Rev. Lett. **99**, 171802 (2007);
[6] T. Aaltonen, *et al* (CDF collaboration), Phys. Rev. Lett. **102**, 031801 (2009)
[7] Z. Sullivan, Phys. Rev. D66, 075011 (2002)